

Comparison of the structure of ribosomal 5S RNA from *E. coli* and from rat liver using X-ray scattering and dynamic light scattering

J. J. Müller*¹, T. N. Zalkova², D. Zirwer¹, R. Misselwitz¹, K. Gast¹,
I. N. Serdyuk², H. Welfle¹, and G. Damaschun¹

¹ Zentralinstitut für Molekularbiologie der Akademie der Wissenschaften der DDR, Robert-Rössle-Strasse 10, DDR-1115 Berlin, German Democratic Republic

² Institute of Protein Research, Academy of Sciences of the USSR, Poustchino, Moscow Region, USSR

Received July 16, 1985 / Accepted November 7, 1985

Abstract. The structures of eukaryotic ribosomal 5S RNA from rat liver and of prokaryotic 5S RNA from *E. coli* (A-conformer) have been investigated by scattering methods. For both molecules, a molar mass of $44,500 \pm 4,000$ was determined from small angle X-ray scattering as well as from dynamic light scattering. The shape parameters of the two rRNAs, volume V_c , surface O_c , radius of gyration R_s , maximum dimension of the molecule L , thickness D , and cross section radius of gyration R_{sq} , agree within the experimental error limits. The mean values are $V_c = 57 \pm 3 \text{ nm}^3$, $O_c = 165 \pm 10 \text{ nm}^2$, $R_s = 3.37 \pm 0.05 \text{ nm}$, $L = 10.8 \pm 0.7 \text{ nm}$, $D = 1.57 \pm 0.07 \text{ nm}$, $R_{sq} = 0.92 \pm 0.01 \text{ nm}$.

Identical structures for the *E. coli* 5S rRNA and the rat liver 5S rRNA at a resolution of 1 nm can be deduced from this agreement and from the comparison of experimental X-ray scattering curves and of experimental electron distance distribution functions. The flat shape model derived for prokaryotic and eukaryotic 5S rRNA shows a compact region and two protruding arms. Double helical stems are eleven-fold helices with a mean base pair distance of 0.28 nm. Combining the shape information obtained from X-ray scattering with the information about the frictional behaviour of the molecules, deduced from the diffusion coefficients $D_{20,w}^0 = (5.9 \pm 0.2) \cdot 10^{-7} \text{ cm}^2 \text{ s}^{-1}$ and $(6.2 \pm 0.2) \cdot 10^{-7} \text{ cm}^2 \text{ s}^{-1}$ for rat liver 5S rRNA and *E. coli* 5S rRNA, respectively, a solvation shell of about 0.3 nm thickness around both molecules is determined. This structural similarity and the consensus secondary structure pattern derived from comparative sequence analyses suggest that all 5S rRNAs may indeed have conserved essentially the same type of folding of their

polynucleotide strands during evolution, despite having very different sequences.

Key words: Ribosomal 5S RNA, structure, X-ray scattering, dynamic light scattering

Introduction

The 5S rRNA is a constituent of the large subunit of all ribosomes. About 200 primary sequences have been determined until now (Erdmann et al. 1984). In spite of the low degree of about 20% overall sequence conservation (Delihas and Andersen 1982), a consensus secondary structure pattern of 5S rRNA was derived from comparative sequence analyses. This general secondary structure model is characterized by five double helices and several single stranded parts in the branching region, in internal loops and hairpin loops. The conservation of this most probable base pairing pattern leads to the question of whether the three-dimensional structures of 5S rRNAs have also been conserved during evolution.

To answer this question, the prokaryotic 5S rRNA from *E. coli* and the eukaryotic 5S rRNA from rat liver were investigated by diffuse X-ray scattering and by dynamic light scattering.

The shape of a 5S rRNA molecule, which is unambiguously determined by the folding of the nucleotide strand, can be obtained from small angle X-ray scattering experiments. Further structural information was obtained from the scattering region at medium scattering angles $5^\circ \leq 2\theta \leq 22^\circ$ which is influenced by the geometry of the secondary structure (Damaschun et al. 1978) as well as by elements of the tertiary structure, as shown for proteins in solution (Fedorov et al. 1976, 1979). Previous in-

* To whom offprint requests should be sent

vestigations of the small-angle X-ray scattering of 5S rRNA from *E. coli* (Connors and Beeman 1972; Österberg et al. 1976; Leontis and Moore 1984), yeast (Connors and Beeman 1972) and rat liver (Müller et al. 1981, 1982) cannot be used for a more detailed analysis, because a comparison of the published structure parameters is not sufficient to prove subtle structural differences. High precision in the measurements is necessary, especially in the medium angle region, which is only attainable if identical diffractometers are used. Furthermore, identical algorithms for data processing and evaluation are essential.

Dynamic light scattering provides the translational diffusion coefficient and the corresponding hydrodynamic Stokes' radius. These parameters, in combination with data from the X-ray scattering experiments allow an independent proof of the results concerning the shape and the dimensions of the macromolecule and allow estimates of its solvation shell.

Materials and methods

Materials

Rat liver 5S rRNA was prepared from the 5S rRNA-protein L5 complex. This complex was obtained by EDTA-treatment of 60S ribosomal subunits or mixtures of 40S and 60S subunits as described earlier (Behlke et al. 1980) and deproteinized by phenol/sodium dodecyl sulphate. 5S rRNA was further purified by gel filtration on Sephadex G-100 in 1 M sodium chloride. The purity of 5S rRNA was demonstrated by gel electrophoresis in 10% polyacrylamide in a buffer system of 90 mM Tris, 2.5 mM EDTA, 90 mM boric acid, pH 8.3. For further characterization, the 5S rRNA was dissolved in 5 mM Tris-HCl, pH 7.8, 50 mM KCl, 1.5 mM MgCl₂, 5 mM 2-mercaptoethanol (ionic strength about 0.07 M).

The prokaryotic *E. coli* 5S rRNA (A-conformer) was prepared from *E. coli* MRE 600 by the method of Erdmann et al. (1971) with slight modifications. Bulk rRNA was obtained from 70S ribosomes by phenol/sodium dodecyl sulphate deproteinization. The rRNA was fractionated by gel filtration on Sephadex G-100 (5 × 100 cm column) in 0.02 M Tris-HCl, pH 7.5, 0.75 M NaCl, 0.002 M EDTA, 1% (v/v) methanol. The peak fraction of 5S rRNA was rechromatographed on Sephadex G-100 (2.5 × 100 cm column) in the same medium. The purity of the 5S rRNA was controlled by gel electrophoresis in 10% polyacrylamide as described for rat liver 5S rRNA. For the scattering experiments the *E. coli* 5S rRNA

was dissolved in 10 mM sodium cacodylate, pH 7.0, 50 mM NaCl, 4 mM MgCl₂.

Concentrations were determined from the absorbance at 260 nm using $A_{1\text{cm}}^{0.1\%} = 21.4$ (Österberg et al. 1976).

Methods

X-ray scattering. Small angle X-ray scattering experiments were made with a highly stabilized X-ray generator (Freiberger Präzisionsmechanik, Freiberg, GDR) using a 1.5 KVA copper tube. The scattered intensities were recorded stepwise with a Kratky-diffractometer (Anton Paar KG, Graz, Austria) for $0.0782 \leq s \text{ (nm}^{-1}\text{)} \leq 5.6$ and with a four-slit diffractometer for $0.142 \leq s \text{ (nm}^{-1}\text{)} \leq 15.55$ ($s = 4\pi \lambda^{-1} \sin \theta$; 2θ , scattering angle; λ , wavelength of the X-rays). The radiation was monochromatized by pulse-height discrimination and by a nickel- β -filter, and the scattering intensities were measured with a proportional counter (Kratky-diffractometer) or a scintillation counter (four-slit diffractometer). The absolute scattered intensities were determined using the standard Lupolen 1811 M (Pilz 1969). The concentrations of *E. coli* 5S rRNA samples were 110 mg/ml for the medium-angle scattering experiments and 2.2–12.1 mg/ml for small-angle measurements (Fig. 1). The corresponding concentrations of rat liver 5S rRNA were 38 mg/ml and 2.7–11.3 mg/ml (Fig. 2). The X-ray experiments were performed at 4 °C. Repeated measurements

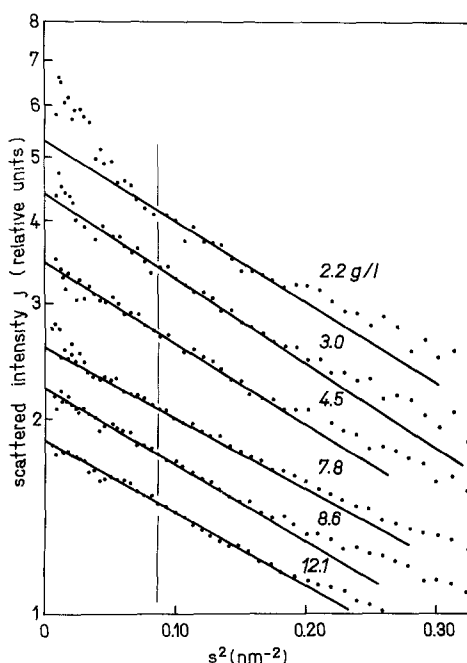


Fig. 1. Guinier plot of the collimation distorted scattered intensity from *E. coli* 5S rRNA (A-conformer) for various concentrations. The vertical line marks the first sampling point

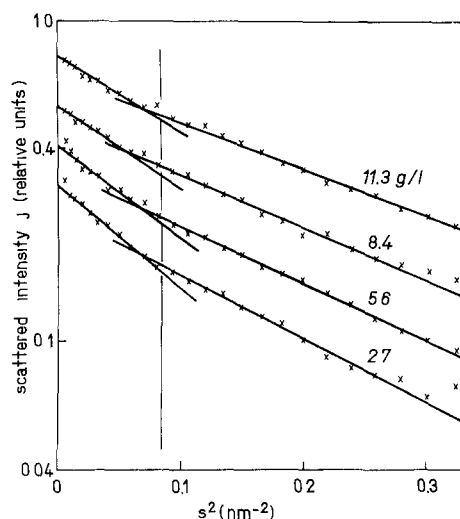


Fig. 2. Guinier plot of the collimation distorted scattered intensity from rat liver 5S rRNA for various concentrations. The vertical line marks the first sampling point. The proximal parts of the scattering curves are influenced by oligomers

proved that the scattering behaviour of the samples did not change during the experiments and electrophoretic controls after X-ray measurements showed that the 5S rRNA remained intact. The scattering data for both 5S rRNA species were treated identically by direct methods (Müller et al. 1977; Damaschun et al. 1978). Reduction of statistical errors, of concentration effects, collimation corrections, and the calculation of the distance distribution function $D(x)$ (Damaschun et al. 1978) were performed by the computer program system SAXS. The correction for the scattering of oligomers was done using the sampling theorem extrapolation method (Damaschun and Pürschel 1971; Müller et al. 1977).

Dynamic light scattering. The spectrometer for the dynamic light scattering experiments has been described previously (Gast et al. 1979, 1982). We used an argon-ion laser (ILA120, Carl Zeiss Jena, GDR) at $\lambda_0 = 514.5$ nm. The measurements were performed in the photon-counting homodyne autocorrelation mode at $20.0 \pm 0.1^\circ\text{C}$ and at a constant scattering angle of 90° within the concentration range of 1–8 mg rRNA/ml. Refractive indices were measured with an Abbé refractometer (Carl Zeiss Jena, GDR). Buffer viscosities were determined by an Ubbelohde viscometer and a digital density measuring device DMA 02-A (Anton Paar KG, Graz, Austria). We used specially manufactured scattering cells, so that the sample volume could be minimized to 0.1 ml. After placing the solution in the cell, the cell was tightly closed and centrifuged for 45 min at $3,000 \times g$ and 20°C to remove dust from the scattering volume. However,

our experimental autocorrelation functions always consisted of two well-separable exponentials. The prominent fast component corresponds to monomeric rRNA molecules, whereas we assume that the slow component is due to minor traces of large rRNA-aggregates. Data evaluation was done either by fitting the experimental autocorrelation function with the sum of two exponentials or by performing the inverse Laplace transformation of the autocorrelation function using the computer program CONTIN-VERSION 2 DP (August 1982) of Provencher (1982). The translational diffusion coefficients corresponding to the fast component of the autocorrelation functions were corrected to standard conditions (20°C , water as solvent) and extrapolated to zero rRNA concentration to determine $D_{20,w}^0$. The hydrodynamic Stokes' radii, R_{St} , were calculated via the Stokes-Einstein relation

$$R_{St} = k_B T / 6 \pi \eta D_{20,w}^0,$$

where k_B is Boltzmann's constant, T the absolute temperature ($^\circ\text{K}$) and η the viscosity of water at 20°C .

Results

Figures 1 and 2 show the inner parts of the slit smeared scattering curves for 5S rRNA from *E. coli* and for 5S rRNA from rat liver as Guinier plots.

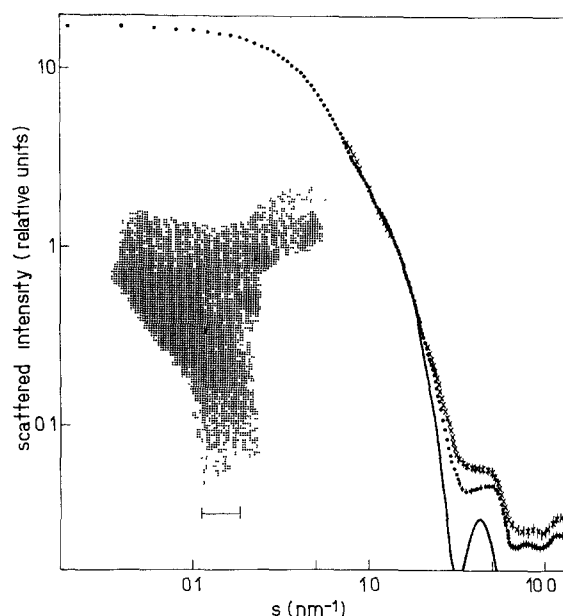


Fig. 3. Corrected experimental scattering curves of 5S rRNA from *E. coli* (···), rat liver (xxx) and theoretical scattering curve of the inserted shape model (—). The length of the horizontal bar is 1 nm. The experimental errors are indicated by vertical bars

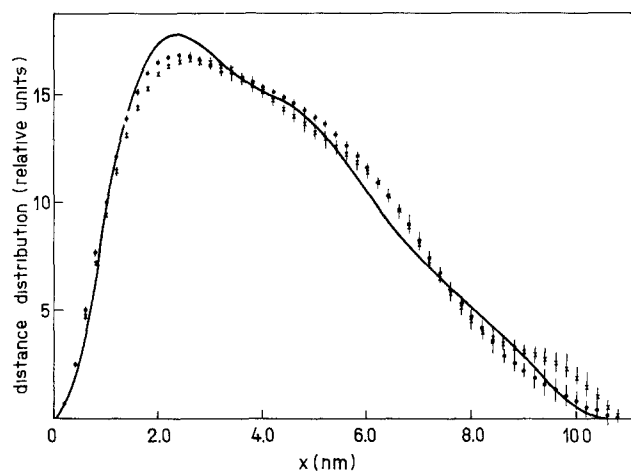


Fig. 4. Electron distance distribution functions of 5S rRNA from *E. coli* (···), rat liver (xxx) and the theoretical function (—) of the shape model (insert in Fig. 3)

Table 1. Structural parameters of rat liver 5S rRNA and *E. coli* 5S rRNA

Parameter	Rat liver	<i>E. coli</i>
Molar mass M [g mol ⁻¹] ^c	45,000 ± 4,000	44,000 ± 4,000
Shape volume V_s [nm ³]	58 ± 3	56 ± 3
Shape surface O_s [nm ²]	169.5 ± 10	161 ± 10
Radius of gyration		
$R_{s,G}$ [nm] ^a	3.31 ± 0.06	3.27 ± 0.05
$R_{s,p}$ [nm] ^b	3.42 ± 0.06	3.31 ± 0.05
Maximum dimension L [nm]	10.9 ± 0.8	10.8 ± 0.6
Molar mass per unit length $M/\Delta x$ [g mol ⁻¹ nm ⁻¹]	2,600 ± 200	2,570 ± 200
Cross-sectional radius of gyration $R_{sq,2}$ [nm]	0.92 ± 0.02	0.915 ± 0.01
Thickness D [nm]	1.6 ± 0.08	1.53 ± 0.05
Diffusion coefficient $D_{20,0}^0$ [cm ² s ⁻¹]	(5.9 ± 0.2) · 10 ⁻⁷	(6.2 ± 0.2) · 10 ⁻⁷
Stokes' radius R_{St} [nm]	3.6 ± 0.1	3.4 ± 0.1

^a Derived from the Guinier-approximation

^b Derived from the distance distribution function

^c Partial specific volume $\bar{v} = 0.54$ cm³/g

The scattering of oligomers falsifies the proximal parts of both scattering curves. The scattering curves were corrected by omitting the scattered intensity up to about the first sampling point (Damaschun et al. 1978), which is marked by a vertical line in Figs. 1 and 2, and by extrapolating the intensity to zero angle using the sampling theorem extrapolation method (Damaschun and Pürschel 1971; Müller et al. 1977). The desmeared scattering curves (Müller et al. 1977), corrected for scattering from oligomers and for concentration influences, are shown for both rRNA species in Fig. 3. In the small angle region

$s \leq 2.2$ nm⁻¹, there are no significant differences between the two curves. The electron distance distribution functions of both molecules (Fig. 4) were calculated by a Fourier sine transform of the scattered intensity. For this transform, the scattered intensity was continued from $s = 2.2$ nm⁻¹ to infinity by a k/s^4 -tail (Damaschun et al. 1978; Müller et al. 1981). These functions agree very well, too. The error bars were calculated by a direct error propagation procedure from the statistical errors in the primary scattering data.

Several molecular parameters can be calculated (Table 1) from the scattering curves as well as from the electron distance distribution functions (Damaschun et al. 1978). In comparison with recently published values (Müller et al. 1981, 1982), the molar mass M , the shape surface O_s , the radius of gyration R_s , and the maximum dimension L of the rat liver 5S rRNA are somewhat enhanced, which results from the modified correction for the scattering of oligomers. But independent of the kind of correction, the corresponding molecular parameters for the two 5S rRNAs agree within the experimental errors. The small diminution of all parameters of the *E. coli* 5S rRNA (Table 1) in comparison with the parameters of the rat liver 5S rRNA is not significant. The correction procedure effects small changes in the values of the molecular parameters, but not in the relations of the parameters for the two rRNA species.

Both scattering curves as well as the electron distance distribution functions (Figs. 3 and 4) were approximated by the corresponding curves calculated for the homogeneous shape model shown in Fig. 3. It can be deduced from the so-called model resolution function (Müller et al. 1985b) that the structures of both molecules and of the model are identical at a resolution of about 1.0 nm (Damaschun et al. 1978). Minor variations of the shape, consistent with the resolution attained, have recently been discussed (Müller et al. 1985b).

In the medium-angle region $2.2 \leq s$ (nm⁻¹) ≤ 15.5 , the scattered intensities are somewhat different for the two rRNA species. Besides the statistical errors shown in Figs. 3 and 5, there possibly exist systematic errors arising from the background correction (Damaschun et al. 1978). These errors can be nearly of the same order of magnitude as the differences between the scattering curves of both 5S rRNAs in the region $s \sim 6$ nm⁻¹ (Fig. 3). However, the errors merely cause a vertical shift of the scattering curve in this angular region without changes in the positions of the maxima.

From the positions of the maxima in the medium-angle regions of scattering curves, we get mainly information about geometrical parameters of double

helical stems in the rRNA molecules. Comparison of the experimental curve of rat liver 5S rRNA with the theoretical scattering curve of double helical oligonucleotides calculated from atomic coordinates (Müller 1983) revealed that the nucleotide pairs are structurally organized as in the A-form double-helix, defined by Arnott et al. (1972), with a mean turn angle of 32.7° and a mean distance $\Delta z = 0.28$ nm between the base pairs (Müller et al. 1985a). The double helical regions of *E. coli* 5S rRNA are also arranged in the A-form double helix as can be concluded from the comparison of the positions of the maxima in the experimental curves of 5S rRNA and in the theoretical scattering curve of an oligonucleotide shown in Fig. 5. We know from experimental data (Table 2) and from computer simulations that for small RNA molecules with short stems or arms, the influence of the packing of these elements on the medium-angle scattering is small, so that the scattering from the secondary structure elements is not significantly distorted.

Figure 6 shows the dependence of the translational diffusion coefficients $D_{20,w}$ on concentration for both 5S rRNA species. From extrapolations to zero concentration, we obtain the diffusion coefficients $D_{20,w}^0 = (5.9 \pm 0.2) \times 10^{-7} \text{ cm}^2 \text{ s}^{-1}$ and $D_{20,w}^0 = (6.2 \pm 0.2) \times 10^{-7} \text{ cm}^2 \text{ s}^{-1}$ as well as the corresponding Stokes' radii $R_{St} = 3.6 \pm 0.1$ nm and $R_{St} = 3.4 \pm 0.1$ nm for rat liver 5S rRNA and *E. coli* 5S rRNA, respectively. Our value of the diffusion coefficient for *E. coli* 5S rRNA is very close to the value $D_{20,w} = 6.27 \times 10^{-7} \text{ cm}^2 \text{ s}^{-1}$ determined by Kao and Crothers (1980) for the compact state ("high-temperature" A-form) of *E. coli* 5S rRNA. The difference of about 5% between the diffusion coefficients for the two 5S rRNA species cannot be regarded as significant since the error limits of the two values overlap (Fig. 6).

We calculated the molar masses of the 5S rRNAs via the Svedberg equation $M_{s,D} = RTs/[D(1-\bar{v}\rho)]^{-1}$, where R is the gas constant, T the absolute temperature, s the sedimentation coefficient, \bar{v} the partial specific volume, and ρ the solvent density. We used the diffusion coefficients determined by us and data from the literature for $\bar{v} = 0.54 \text{ cm}^3 \text{ g}^{-1}$ (Österberg et al. 1976) and $s = 5.3 \text{ S}$ (*E. coli*, Fox and Wong 1982) and $s = 4.9 \text{ S}$ (rat liver, Behlke et al. 1980), respectively. We obtained molar masses $M_{s,D} = 45,000 \pm 4,000 \text{ g mol}^{-1}$ for *E. coli* 5S rRNA and $M_{s,D} = 44,000 \pm 4,000 \text{ g mol}^{-1}$ for rat liver 5S rRNA. These values are entirely consistent with the molar masses determined from the X-ray scattering data.

Furthermore, the diffusion coefficients can be calculated semi-empirically using only X-ray scattering data (Kumosinski and Pessen 1982; Müller

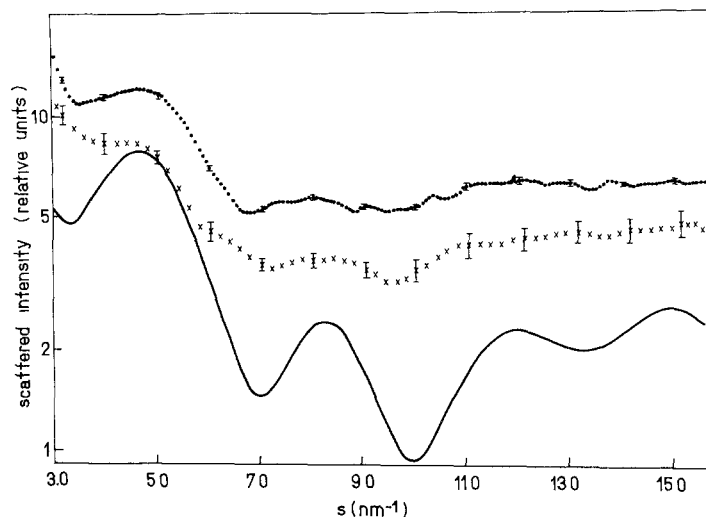


Fig. 5. Smoothed medium-angle scattering curves of 5S rRNA from *E. coli* (···), rat liver (×××) and theoretical scattering curve (—) calculated from the atomic coordinates of an octamer with alternating base pairs A-U and G-C arranged in an A-form double helix (Müller 1983). The curves are shifted vertically by an arbitrary value for clarity

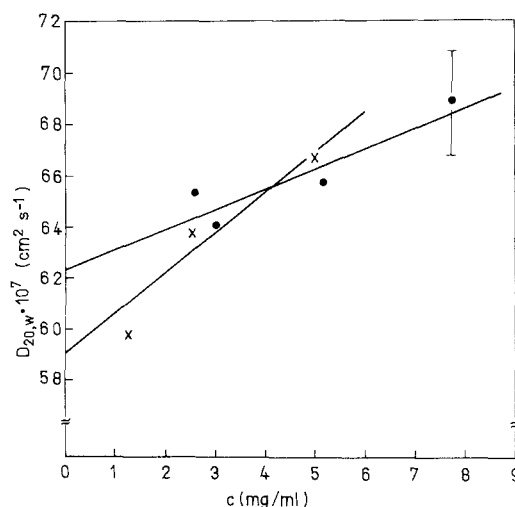


Fig. 6. Concentration dependence of the diffusion coefficients $D_{20,w}$ for 5S rRNA from *E. coli* (•) and from rat liver (×). The bar shown indicates the error limits of the experimental values

Table 2. Positions of the subsidiary maxima in the medium angle region of experimental and theoretical scattering curves

	$s \text{ (nm}^{-1}\text{)}$	
	First maximum	Second maximum
5S rRNA rat liver	4.6 ± 0.1	8.25 ± 0.1
5S rRNA <i>E. coli</i>	4.7 ± 0.1	8.0 ± 0.1
tRNA ^{Phe}	4.75 ± 0.1	8.25 ± 0.1
(Müller et al. 1982)		
5.8S rRNA rat liver	4.55 ± 0.1	8.4 ± 0.1
(Müller et al. 1985)		
(A-G) ₄ · (C-U) ₄	4.65	8.3
A-form RNA		

et al. 1984). The values are determined from the experimental shape parameters V_c , O_c/V_c , $R_{s,p}$ and from the molar mass M to be $D_{\text{calc}} = 5.93 \times 10^{-7} \text{ cm}^2 \text{ s}^{-1}$ and $6.1 \times 10^{-7} \text{ cm}^2 \text{ s}^{-1}$ for rat liver and *E. coli* 5S rRNA, respectively. These calculated values agree very well with the experimental results from dynamic light scattering, demonstrating the consistency of the results from both experimental methods.

A combination of data from X-ray scattering (shape and dimensions) and dynamic light scattering (diffusion coefficient) allows us to estimate the size of the outer solvation shell of the 5S rRNA molecules. The Stokes' radius of the shape model (Fig. 3), which is common to both 5S rRNA species, can be calculated (Müller et al. 1983) using the approximation of Kirkwood and the shell theory of Bloomfield (Teller et al. 1979) to be $R_{Sf, \text{calc}} = 3.2 \text{ nm}$. The difference between this value and the experimental Stokes' radii $R_{Sf} = 3.6 \text{ nm}$ and $R_{Sf} = 3.4 \text{ nm}$ for 5S rRNA from rat liver and *E. coli*, respectively, corresponds to the mean thickness of the solvation shell fixed to the surface of the molecules. Assuming a uniform distribution around the shape model, we get a mean thickness of about 0.3 nm for the outer solvation shell.

Discussion

We have shown that the dimensions (Table 1), the shape and the solvation shell of 5S rRNA molecules from *E. coli* and rat liver are very similar at a structure resolution of 1.0 nm and within the error limits of our measurements. The inner structure of double-helically organized regions of the pro- and eukaryotic 5S rRNA molecules is also very similar. The mean geometrical parameters of the double helices in both molecules are about 33° for the turn angle and 0.28 nm for the base pair distance. However, local deviations from this averaged structure are possible to the same extent as shown for tRNA^{Phe} (Holbrook et al. 1978). The small differences in the medium-angle region of the scattering curves of *E. coli* 5S rRNA and rat liver 5S rRNA are possibly caused by some minor rearrangements of the nucleotide strand within the shape shown in Fig. 3, rather than by different geometries of secondary structure elements. However, for a consensus secondary structure of pro- and eukaryotic 5S rRNA (Böhm et al. 1982; Delibas and Andersen 1982), the type of folding must also remain conserved.

The agreement of the experimental translational diffusion coefficients for the 5S rRNAs from rat liver and *E. coli*, within the limits of experimental errors, also points to very similar dimensions for the two molecules. The thickness of the solvation shell,

diffusing with the 5S rRNA molecules, is comparable to the value determined for tRNA^{Phe} (Müller et al. 1983). The finding that the shape and dimensions of pro- and eukaryotic 5S rRNA molecules are very similar is consistent with the results of Morikawa et al. (1984) from packing studies of 5S rRNA from *Th. thermophilus*.

Recently determined values of the radius of gyration, $R_g = 3.29 - 3.37 \text{ nm}$, and of the maximum dimension $L = 10.5 \text{ nm}$ for *E. coli* 5S rRNA (Leontis and Moore 1984) agree with our results within the error limits. The radius of gyration determined by Connors and Beeman (1972), $R_g = 3.37 \pm 0.06 \text{ nm}$, is also in agreement with our value. On the other hand, larger dimensions for the 5S rRNA from *E. coli* have been determined by Fox and Wong (1979) from hydrodynamic data, by Österberg et al. (1976) from small angle X-ray scattering and also from electron microscopic images (Pieler et al. 1984). The discrepancies may be explained by limitations of the techniques applied, rather than by different properties of the 5S rRNA samples analyzed. At least the hydrodynamic (Fox and Wong 1979) and small angle X-ray scattering experiments have been performed under ionic conditions which should maintain the 5S rRNA in a compact form in the sense of Kao and Crothers (1980). Our results from small angle X-ray scattering have shown that models whose scattering curves are consistent with the experimental data exhibit invariably a compact core (Fig. 3).

Nazar and Wildeman (1983) have shown that it is impossible to reconstitute complexes between the eukaryotic protein YL3 and prokaryotic 5S rRNA, and Wrede and Erdmann (1973) have demonstrated that eukaryotic 5S rRNA cannot be incorporated into the 50S ribosomal subunit from prokaryotes. Our data show that these findings cannot be explained by fundamental structural differences between pro- and eukaryotic 5S rRNAs. Probably, for the protein binding of 5S rRNA, subtle relations between the positions of double-helical regions of the RNA (Nazar and Wildeman 1983) and/or specific interactions with particular nucleotides are responsible.

In conclusion, the experimental X-ray scattering curves of *E. coli* 5S rRNA and rat liver 5S rRNA as well as the shape (Figs. 3–5) and the molecular dimensions determined from these curves are very similar. Comparative sequence analyses have shown the conservation of the general folding pattern of the polynucleotide strands of 5S rRNAs from many species on the secondary structure level. The similarity of the three-dimensional structures of a prokaryotic and an eukaryotic 5S rRNA, demonstrated in this work, also suggest that the three-dimensional

structures of 5S rRNAs have been conserved with respect to the general features during evolution, in spite of the differences in nucleotide sequences.

References

- Arnott S, Hukins DWL, Dover SD (1972) Optimized parameters for RNA double-helices. *Biochem Biophys Res Commun* 48:1392–1399
- Behlke J, Welfle H, Wendel I, Bielka H (1980) Physicochemical studies of the 7S complex of rat liver ribosomes and its components. *Acta Biol Med Germ* 39:33–40
- Böhm S, Fabian H, Welfle H (1982) Universal structural features of prokaryotic and eukaryotic ribosomal 5S RNA derived from comparative analysis of their sequences. *Acta Biol Med Germ* 41:1–16
- Connors PG, Beeman WW (1972) Size and shape of 5S ribosomal RNA. *J Mol Biol* 71:31–37
- Damaschun G, Pürschel HV (1971) Röntgen-Kleinwinkelstreuung von isotropen Proben ohne Fernordnung. I. Allgemeine Theorie. *Acta Cryst* A27:193–197
- Damaschun G, Müller JJ, Bielka H (1978) Scattering studies of ribosomes and ribosomal components. *Methods Enzymol* 59:706–750
- Delihans N, Andersen J (1982) Generalized structures of the 5S ribosomal RNAs. *Nucleic Acids Res* 10:7323–7344
- Erdmann VA, Doberer HG, Sprinzl M (1971) Structure and function of 5S RNA: The role of the 3' terminus in 5S RNA function. *Mol Gen Genet* 114:89–94
- Erdmann VA, Wolters J, Huysmans E, Vandenbergh A, De Wachter R (1984) Collection of published 5S and 5.8S ribosomal RNA sequences. *Nucleic Acids Res* 12:r133–166
- Fedorov BA, Kröber R, Damaschun G, Ruckpaul K (1976) Experimental and theoretical large-angle X-ray diffuse scattering by globins in solution. Sensitivity of the method. *FEBS Lett* 65:92–95
- Fedorov BA, Timchenko AA, Denesyuk AI, Ptitsyn OB, Damaschun G (1979) Comparative analysis of globular protein structures in crystal and in solution with X-ray diffuse scattering. In: Hofmann E (ed) *Proteins: structure, function and industrial applications*. Pergamon Press, Oxford, pp 153–158
- Fox JW, Wong KP (1979) The hydrodynamic shape, conformation and molecular model of *E. coli* ribosomal 5S RNA. *J Biol Chem* 254:10139–10144
- Fox JW, Wong KP (1982) Acquisition of native conformation of ribosomal 5S ribonucleic acid from *E. coli*. Hydrodynamic and spectroscopic studies on the unfolding and refolding of ribonucleic acid. *Biochemistry* 21:2096–2102
- Gast K, Zirwer D, Fahrenbruch B, Pittelkow R (1979) Eine einfache Meßanordnung für die quasi-elastische Lichtstreuung. *Exp Tech Phys* 27:319–329
- Gast K, Zirwer D, Ladhoff AM, Schreiber J, Koelsch R, Kretschmar K, Lasch J (1982) Auto-oxidation-induced fusion of lipid vesicles. *Biochim Biophys Acta* 686:99–109
- Holbrook SR, Sussman JL, Warrant RW, Kim SH (1978) Crystal structure of yeast phenylalanine transfer RNA. II. Structural features and functional implications. *J Mol Biol* 123:631–660
- Kao TH, Crothers DM (1980) A proton-coupled conformational switch of *E. coli* 5S rRNA. *Proc Natl Acad Sci USA* 77:3360–3364
- Kumosiński TF, Pessen H (1982) Estimation of sedimentation coefficients of globular proteins: An application of small-angle X-ray scattering. *Arch Biochem Biophys* 219:89–100
- Leontis NB, Moore PB (1984) A small angle X-ray scattering study of a fragment derived from *E. coli* 5S RNA. *Nucleic Acids Res* 12:2193–2203
- Monikawa K, Fujiyoshi Y, Ishizuka K, Kawakami M, Take-mura S (1984) Various types of 5S rRNA crystals as studied by X-ray diffraction and electron microscopy. *Nucleic Acids Res* 15:143–146
- Müller JJ (1983) Calculation of scattering curves for macromolecules in solution and comparison with results of methods using effective atomic scattering factors. *J Appl Cryst* 16:74–82
- Müller JJ, Damaschun G, Walter G (1977) Über ein Computer-Programmsystem für die Strukturuntersuchung von Biopolymeren mit Hilfe der Röntgen-Kleinwinkelstreuung. In: *Exp Methoden der Molekülphysik, Physikalische Gesellschaft der DDR, Reinhardtsbrunn*, pp 11–30
- Müller JJ, Welfle H, Damaschun G, Bielka H (1981) Shape and secondary structure of native 5S RNA from rat liver ribosomes. A small angle and wide angle X-ray scattering study. *Biochim Biophys Acta* 654:156–165
- Müller JJ, Damaschun G, Wilhelm P, Welfle H, Pilz I (1982) Comparison of the structures of the native form of rat liver 5S rRNA and yeast tRNA^{Phe}. Small angle and wide angle X-ray scattering study. *Int J Biol Macromol* 4:289–296
- Müller JJ, Glatter O, Zirwer D, Damaschun G (1983a) Calculation of small angle X-ray and neutron scattering curves and of translational coefficients on the common basis of finite elements. *Studia Biophys* 93:39–46
- Müller JJ, Zirwer D, Damaschun G, Welfle H, Gast K, Plietz P (1983b) The translational frictional coefficients of rape seed 11S globulin, tRNA^{Phe} and ribosomal 5S RNA. Calculation on the basis of finite elements. *Studia Biophys* 96:103–108
- Müller JJ, Damaschun H, Damaschun G, Gast K, Plietz P, Zirwer D (1984) Determination of hydrodynamic properties of biopolymers from small angle X-ray scattering data. *Studia Biophys* 102:171–175
- Müller JJ, Misselwitz R, Zirwer D, Damaschun G, Welfle H (1985a) A-form to A'-form conformational switch of double helices in rat liver 5S and 5.8S rRNA. *Eur J Biochem* 148:89–95
- Müller JJ, Damaschun G, Schmidt PW (1985b) The model resolution function – a technique for estimating the quality of approximation of particles by models in small angle X-ray or neutron scattering. *J Appl Cryst* 18:241–247
- Nazar RN, Wildeman AG (1983) Three helical domains form a protein binding site in the 5S RNA-protein complex from eukaryotic ribosomes. *Nucleic Acids Res* 11:3155–3168
- Österberg R, Sjöberg B, Garrett RA (1976) Molecular model for 5S RNA. A small angle X-ray scattering study of native, denatured and aggregated 5S RNA from *E. coli* ribosomes. *Eur J Biochem* 68:481–487
- Pieler T, Digweed M, Erdmann VA (1984) The structure and function of ribosomal 5S rRNAs. In: Clark BFC, Petersen HU (eds) *Gene expression. Alfred Bencon Symposium 19*. Munksgaard, Copenhagen
- Pilz I (1969) Absolute intensity measurements of small angle X-ray scattering by means of a standard sample. *J Colloid Interface Sci* 30:140–144
- Provencher SW (1982a) A constrained regularization method for inverting data represented by linear algebraic or integral equations. *Comput Phys Commun* 27:213–227
- Provencher SW (1982b) CONTIN: A general purpose constrained regularization program for inverting noisy linear algebraic and integral equations. *Comput Phys Commun* 27:229–242
- Wrede P, Erdmann VA (1973) Activities of *B. Stearotherophilus* 50S ribosomes reconstituted with prokaryotic and eukaryotic 5S RNA. *FEBS Lett* 33:315–319
- Teller DC, Swanson E, De Haen CH (1979) The translational friction coefficient of proteins. *Methods Enzymol* 61:103–124